AIAA 2002-0943

Meteorology Associated with Turbulence Encounters During NASA's Fall-2000 Flight Experiments

David W. Hamilton and Fred H. Proctor
NASA Langley Research Center
Hampton, VA

40th Aerospace Sciences Meeting & Exhibit
January 14-17, 2002
Reno, Nevada

AIAA-2002-0943

METEOROLOGY ASSOCIATED WITH TURBULENCE ENCOUNTERS DURING NASA'S FALL-2000 FLIGHT EXPERIMENTS

David W. Hamilton* and Fred H. Proctor†
NASA Langley Research Center
Hampton, Virginia

Abstract

Initial flight experiments have been conducted to investigate convectively induced turbulence and to test technologies for its airborne detection. Turbulence encountered during the experiments is described with sources of data measured from in situ sensors, ground-based and airborne Doppler radars, and aircraft video. Turbulence measurements computed from the in situ system were quantified in terms of RMS normal loads ($\sigma_{\Delta n}$), where 0.20 g $\leq\sigma_{\Delta n}\leq$0.30 g is considered moderate and $\sigma_{\Delta n}$ > 0.30 g is severe. During two flights, 18 significant turbulence encounters ($\sigma_{\Delta n}\geq$0.20 g) occurred in the vicinity of deep convection; 14 moderate and 4 severe. In all cases, the encounters with turbulence occurred along the periphery of cumulus convection. These events were associated with relatively low values of radar reflectivity, i.e. RRF < 35 dBz, with most levels being below 20 dBz. The four cases of severe turbulence occurred in precipitation and were centered at the interface between a cumulus updraft turret and a downwind downdraft. Horizontal gradients of vertical velocity at this interface were found to be strongest on the downwind side of the cumulus turrets. Furthermore, the greatest loads to the aircraft occurred while flying along, not orthogonal to, the ambient environmental wind vector. During the two flights, no significant turbulence was encountered in the clear air (visual meteorological conditions), not even in the immediate vicinity of the deep convection.

Corroboration of ground based and airborne radar spectrum width calculations support the in situ derived normal loads experienced during the most severe encounter. However, the available ground based radar data did not predict most of the encountered events.

Introduction

Sudden and unexpected encounters with turbulence have led to frequent injuries aboard commercial aircraft. Many of these turbulence accidents were found to be near or within convective activity.[1] Therefore, the National Aeronautics and Space Administration, through its Aviation Safety Program, is addressing turbulence hazards through research, flight experiments, and data analysis. Primary focus of this program element is the characterization of turbulence and its environment, as well as the development and testing of hazard-estimation algorithms for both radar and *in situ* detection. The ultimate goal is to operationally test sensors that will provide ample warning prior to hazardous turbulence encounters. In order to collect data for support of these activities, NASA-Langley's B-757 aircraft was directed into regions favorable for Convectively-Induced Turbulence (CIT). In this paper, we describe the environment and the turbulence encountered during the flights using data collected from the aircraft, ground-based Doppler radar, and standard meteorological data.

An extensive review of the literature describing the causes for CIT can be found in Pantley[2]. In his thesis he presents the types of CIT considered hazardous to aircraft: 1) updrafts and downdrafts within and on the periphery of deep cumulus convection, 2) rapidly growing thunderstorms that may go undetected by airborne weather radar, 3) Kelvin-Helmoltz instability induced by thunderstorm outflows along the tropopause, 4) turbulent vortices that form due to the breaking of convectively triggered atmospheric waves above and downwind of thunderstorms, and 5) turbulent wakes caused by barrier type effects around and in the lee of thunderstorms. During NASA's flight experiments,

*Research Scientist, Airborne Systems Competency
†Research Scientist, Airborne Systems Competency, AIAA member

turbulence was encountered near the tops of growing cumulus turrets, like that of types 1 and 2 listed above.

The presence of hazardous turbulence within strong, rapidly-growing thunderstorms is well known.[3,4] Accidents continue to occur near thunderstorms although in many cases they are attributed to factors other than encountering the convective drafts associated with the thunderstorm.[5,6,7,8] Some encounters near convection may even be labeled as clear air turbulence (CAT). Wingrove and Bach describe an accident case near Bermuda on October 12, 1983 where an aircraft was reported to have experienced severe CAT resulting in 12 injuries. Although the event was denoted as 'clear air', the pilot reported that the aircraft was flying through the top of a growing cumulonimbus cloud at the time of the encounter. In this event the aircraft experienced a peak normal load (n) of -1.58 *g* upon exiting of the cumulus updraft. The airborne radar was reported to have detected no precipitation within the cloud and the event was therefore denoted as CAT.

Another case where a possible encounter with convection was attributed to CAT is in Pantley and Lester[8] (PL). In this event, which occurred over Hannibal, MO on April 4, 1981, the aircraft experienced severe turbulence while in cruise near the tops of thunderstorms. PL claim that the accident was caused by the presence of a three-dimensional wake located downstream of an overshooting top. However, the pilot report states that the aircraft was operating within a thin cirrus cloud. Upon exiting of the cirrus, the aircraft 'encountered a second "clearly formed cloud" that was illuminated "by a lightning flash off to the side and below."' This report further adds to the suspicion that some encounters attributed to CAT are really encounters with low reflectivity thunderstorm tops.

Attempts have been made to identify CIT from ground-based radar.[6,9,10,11] In early works, both Press and Binkley[9] and Thompson and Lipscomb[10] found that turbulence encounters near thunderstorms can be reduced by avoiding radar echo regions. However, avoiding these regions is not always possible. Furthermore, some accidents may still occur outside of the radar echo regions associated with thunderstorms[6]. With the introduction of Doppler radar, turbulence can be detected using the spectrum width[11]. Lee[12] has shown that there is a good agreement between the spectrum width from ground-based radar and aircraft penetration measurements of turbulence velocity when the aircraft was within 1 *km* of the radar resolution volume. Furthermore, Lee found that within regions of moderate or severe turbulence the spectrum width exceeded 5 ms^{-1}. However, the spectrum width calculations may not be accurate if the radar reflectivity is weak or if the event is at a range greater than 60 *km* from the radar[13]. Older technology airborne weather radars were limited in capability to detect and quantify aircraft turbulence hazards. However, current generation radars with predictive wind shear (PWS) capability offer new opportunities. Bowles[14,15] has provided a technical basis for relating aircraft RMS normal loads to airborne radar observables. This paper will briefly examine how the spectrum width from ground based radar compared with flight data.

The Flight Experiments

The initial flight experiments were conducted during November and December of 2000. The aircraft, a B-757, was equipped with *in situ* sensors for wind, temperature and acceleration measurements[16], and an airborne Doppler radar for forward-looking turbulence detection. During these flights, both radar and *in situ* data were collected for events ranging from smooth air to severe turbulence. Direct penetrations into regions with moderate to high reflectivity (RRF > 35 *dBz*) were purposefully avoided at all times during the flights. Commercial carriers routinely avoid these regions, as well.

Flight days were chosen based on the likelihood of CIT somewhere within flight range of NASA Langley. The flight range included most of southeastern US, excluding Texas and south Florida. General locations favorable for CIT were chosen based on real-time weather predictions from the Forecast Systems Lab's (FSL) Rapid Update Cycle (RUC)[17] and Mesoscale Analysis and Prediction System (MAPS)[17] and the National Center for Environmental Prediction's ETA[18,19] models, as well as from a mesoscale-weather prediction model (Mesoscale Atmospheric Simulation System, MASS[20]). The latter was run on a NASA owned workstation and provided key indices for real-time turbulence prediction.

Two flight days in which significant turbulence was encountered are presented. A summary of the two flights is shown in Table 1. Briefly described are the weather conditions and the flight paths for each day. A select number of cases are discussed in detail, with information from airborne and ground-based Doppler radars, as well as data collected from the *in situ* sensor. Ground based radar data (WSR-88D) was acquired from Fort Polk, Louisiana (POE) for the first flight and Tallahassee, Florida (TLH) for the second. Details of wind recovery methods and load estimations from the *in situ* recorder

Table 1. Summary of Turbulence Flight Days

Flight/Day	Weather	Primary Region of Interest	Peak Storm Tops	Cell Motion	Number of Events with Significant Turbulence	Peak In Situ Turbulence $\sigma_{\Delta n}$
190/ 13 Dec 2000	Broad Area of Rain and Convective Cells with Embedded Thunderstorms	Northeast Louisiana	13.7 *km*	35 ms^{-1} (69 *kts*) from 225°	13	0.35
191/ 14 Dec 2000	Narrow Line of Convective Cells/ Thunderstorms	Florida Panhandle & South Georgia	12.2 *km*	13 ms^{-1} (25 *kts*) from 240°	5	0.44

Table 2. Summary of Significant Turbulence Events

Event	Altitude (MSL) *feet*	Peak In Situ Turbulence $\sigma_{\Delta n}$	Δn (*g's*) Max	Δn (*g's*) Min	Peak Vertical Wind (ms^{-1}) Max	Peak Vertical Wind (ms^{-1}) Min	Horizontal Scale (*km*)/ Duration of Event (*sec*)	Peak Radar Reflectivity (near path) airborne/ground
190.1	24,000	0.25	0.41	-0.49	6.85	-4.48	2.2 / 10	16 / 13
190.2	24,000	0.24	0.47	-0.68	4.58	-5.73	6.0 / 28	12 / 13
190.3	24,000	0.20	0.41	-0.49	3.50	-4.19	6.5 / 30	12 / 8
190.4a	24,000	0.24	0.44	-0.58	7.01	-5.34	3.2 / 15	16 / 13
190.4b	24,000	0.28	0.48	-0.77	8.06	-6.71	3.7 / 17	16 / 18
190.4c	24,000	0.26	0.56	-0.44	12.15	-6.53	5.0 / 23	16 / 18
190.5	24,000	0.21	0.53	-0.36	9.71	-2.30	2.2 / 10	16 / 2
190.6	24,000	0.33	0.48	-0.81	9.48	-3.37	2.6 / 12	16 / 8
190.7	24,000	0.35	0.51	-1.22	11.18	-6.23	2.4 / 11	8 / 8
190.8a	24,000	0.20	0.63	-0.33	7.30	-4.45	1.5 / 7	8 / 8
190.8b	24,000	0.22	0.57	-0.46	9.56	-0.62	2.2 / 10	12 / 8
190.8c	24,000	0.22	0.69	-0.26	10.42	0.49	2.0 / 9	16 / 13
190.8d	24,000	0.25	0.62	-0.50	8.49	-1.89	3.7 / 17	12 / 18
191.1a	33,000	0.34	0.95	-0.58	6.05	-15.0	4.2 / 18	12 / NA
191.1b	33,000	0.25	0.54	-0.87	8.36	-8.05	2.8 / 12	20 / NA
191.1c	33,000	0.24	0.78	-0.48	9.32	-2.63	3.4 / 15	16 / NA
191.2	33,000	0.20	0.54	-0.50	6.82	-5.93	18.9 / 80	12 / NA
191.3	33,000	0.44	0.83	-1.40	18.41	-14.9	5.2 / 22	28 / 33

NA – Not Available

can be found in reference 16. The *in situ* turbulence measurements were quantified in terms of the peak normal load acceleration (Δn) and the root mean square (RMS) of the normal load acceleration, $\sigma_{\Delta n}$.[16] Measurements of $\sigma_{\Delta n}$ exceeding 0.3 constitutes severe turbulence and is equivalent to peak normal load accelerations (Δn) exceeding one *g*.[21,22] An event was classified as significant turbulence if it was moderate or worse, i.e. $\sigma_{\Delta n} \geq 0.20$.

Details of the 18 significant turbulence events are listed in Table 2. The events were characterized by large horizontal gradients of vertical velocity along the flight path within rising cumulus plumes or precipitation shafts, which produced the hazardous aircraft loads. Duration of the events was brief, lasting several seconds to a minute and coincides with the time the aircraft was operating in-cloud. The values of radar reflectivity (as derived from the airborne and ground-based radars) were weak with peak values for each event ranging from 8 to 33 *dBz* (Table 2).

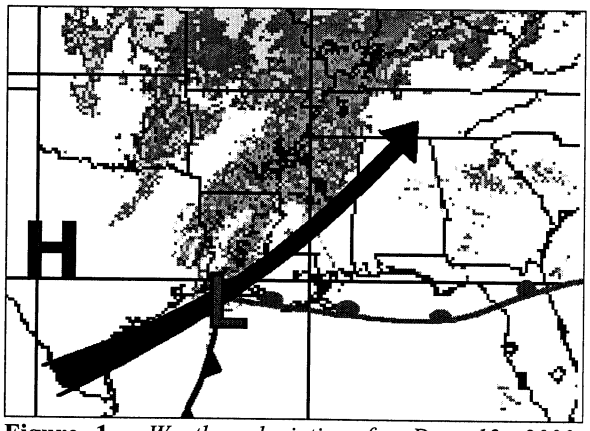

Figure 1. *Weather depiction for Dec. 13, 2000. Depiction shows surface fronts, NWS radar composite (shading), and jet stream position (bold arrow).*

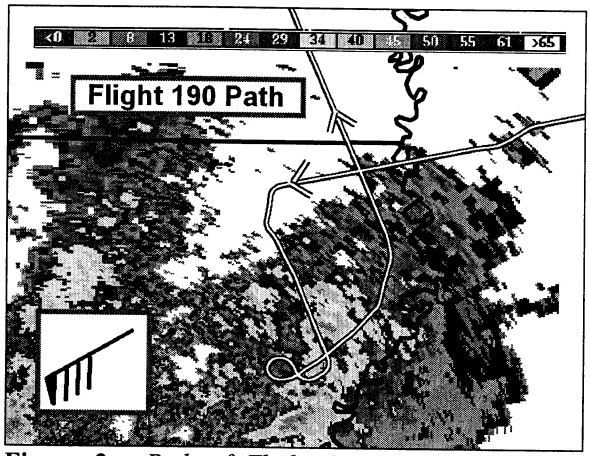

Figure 2. *Path of Flight 190 and ground based composite radar reflectivity (dBz) from the Fort Polk, LA radar at 18:57:48 UTC. Flight level wind vector (knots) is in the inset.*

Flight 190

On December 13, 2000 NASA's B-757 investigated a thunderstorm complex near the Louisiana/Mississippi Gulf Coast. Early in the morning, moderate turbulence had been reported over Louisiana in the vicinity of rapidly building thunderstorms. In the 1800 UTC National Weather Service surface analysis, a low pressure was located near the southwest coast of Louisiana with a warm front extending eastward over the northernmost Gulf of Mexico into central Florida (see Figure 1). A cold high pressure was in place over New England and covered much of the eastern United States. An inverted ridge associated with the high pressure extended east of the Appalachian Mountains with the ridge axis turning southwest through the Gulf Coast States. Very moist, warm tropical air was being driven northward towards the warm front and over the cold high pressure. A sharp temperature gradient was present just north of the warm front with ship and buoy temperatures up to 80°F (27°C) in the tropical air south of the front and 30°F (-1°C) with freezing drizzle reported in Memphis, Tennessee north of the front. Overcast conditions and precipitation were present over much of the Mississippi and Ohio River Valleys with the general cloud tops at about 6.7 *km* (22,000 *ft*) above mean sea level (MSL). Embedded strong thunderstorms surrounded by weaker convection was occurring in northeastern Louisiana and central Mississippi. The thunderstorms, located north of the warm front, had cloud tops with extensive outflow anvils at 13.7 *km* (45,000 ft) MSL. Storm motion as deduced from POE radar imagery was about 35 ms^{-1} (69 *kts*) toward the northeast (from 225°). A midlevel mesoscale shortwave trough and associated jet streak were propagating over Louisiana, thus potentially enhancing convective destabilization. The jet streak maximum was located over the Gulf Coast of Louisiana at 12 *km* (~200 *mb* pressure level) MSL with peak winds of 50 ms^{-1}. Severe thunderstorm warnings were issued later in the day including a warning for one of the larger thunderstorms that the aircraft had been operating near.

The flight path relative to the Fort Polk, Louisiana (POE) radar composite for Flight 190 is shown in Fig. 2. The aircraft was operating in mostly clear air, i.e. visual meteorological conditions (VMC) at 7.3 *km* (24,000 *ft*) MSL, well beneath the anvil outflow of the thunderstorm complex located east of the flight path. Cumulus turrets containing ice crystals and light snow emanated from a stratiform cloud region that was present at lower elevations. A small number of the isolated turrets were located well west of the large thunderstorm complex. Closer to the thunderstorm, the turrets became more numerous and appeared to be merging with the complex. The turbulence encounters resulted from the penetration of the turrets located upwind of the large thunderstorm. Snow and ice crystals within the turrets went nearly undetected by the airborne radar and was later confirmed by the radar at POE to have weak reflectivity with values generally less than 10 *dBz*. Unfortunately, during this flight the POE radar did not detect the spectrum widths associated with each event. Weak radar reflectivity associated with the convection as well as the distance (~170 km) from the radar site might have contributed to the lack of detection[13]. Data from other nearby radar sites in the vicinity of the encounters were not available for the analysis. Therefore, it is not known whether these sites might have detected the turbulence regions.

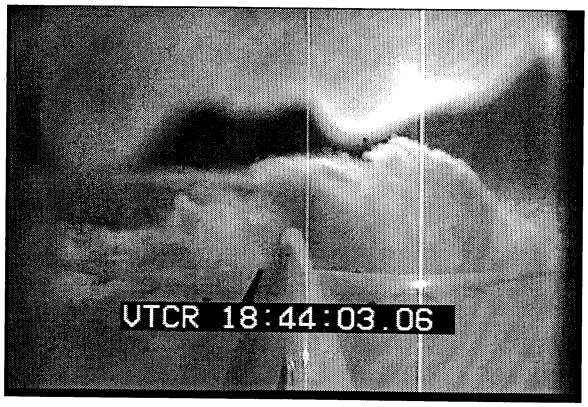

Figure 3. *Aircraft video image at 18:44:03.06 UTC during Flight 190. Image is of a cumulus turret 10 seconds prior to penetration during Event 190.1.*

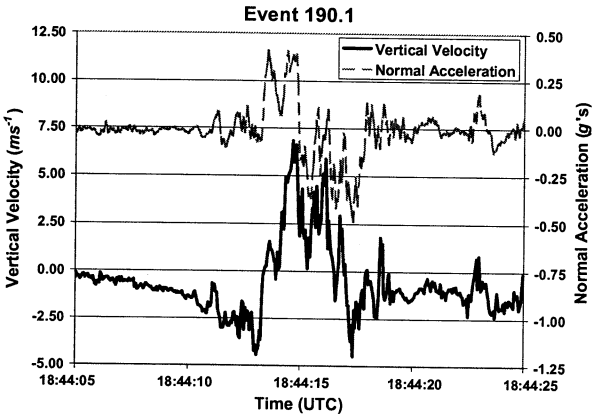

Figure 4. *Plot of Vertical Velocity (solid line in ms^{-1}) and Normal Acceleration at the center of gravity (dotted line in g's) for Event 190.1.*

Specific turbulence events during flight 190 are shown in Figs. 3-7. The events ranged from moderate to severe. A brief description of three of these events follows.

Event 190.1

The first turbulence encounter, 190.1, occurred as the aircraft flew through the top of a rising cumulus plume. Refer to Table 2 for the resulting loads, vertical winds, and radar reflectivity associated with each encounter. The aircraft was flying in VMC in a region of relatively smooth air prior to the penetration of the plume (see Figs. 3 and 4). The aircraft heading was about 150° (0° being true north) and nearly orthogonal to the environmental wind vector (from 240°) as it approached the plume. Wind measurements derived from the *in situ* sensors revealed steep along-track gradients of vertical velocity on the periphery of the plume (See Fig. 4 between 18:44:13

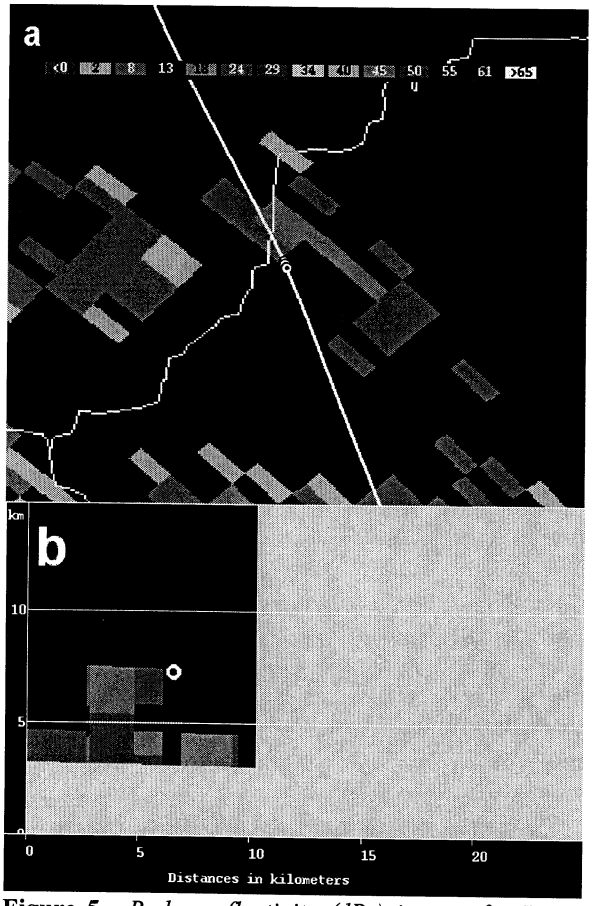

Figure 5. *Radar reflectivity (dBz) images for Event 190.1. Plan view image (a) is the 18:43:08 UTC, 1.4 degree elevation scan from the Fort Polk (POE) radar. Image is about 1 minute prior to and at an altitude 1 km below the aircraft encounter with turbulence (denoted by the circle). The vertical cross section (b) is along the flight path in (a).*

and 18:44:15 UTC). Updraft speeds up to 7 ms^{-1} in the center of the plume and downdrafts outside of the plume of nearly 4.5 ms^{-1} were associated with the turbulence.

The corresponding ground based radar images for case 190.1 are shown in Fig. 5. The maximum radar reflectivity within the cell was 20.5 *dBz* and 13 *dBz* at the location of the encounter. For comparison, the airborne radar detected a maximum reflectivity of 16 *dBz* along the flight path (not shown). The top of the isolated cell is very close to the flight level, i.e. 7.3 *km* (24,000 *ft*), as seen in the radar cross section (Fig. 5b) and in aircraft video (Fig. 3).

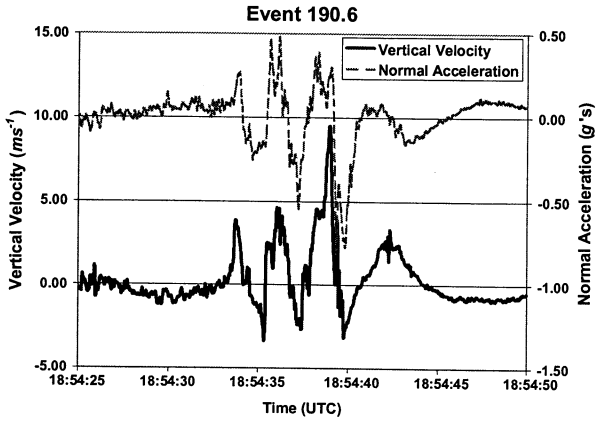

Figure 6. *Same as Fig 3. but for Event 190.6.*

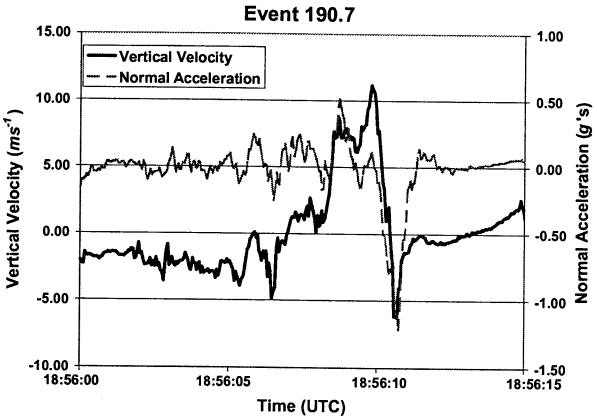

Figure 7. *Same as Fig 3 but for Event 190.7.*

Event 190.6

Event 190.6 was the first of two severe turbulence encounters of the day. The flight path was along the direction of the environmental wind and about 43 *km* (23 *nm*) upstream of the main thunderstorm cell. This event was characterized by the penetration of cumulus turrets on the flanks of the larger thunderstorm cell. Just as in Event 190.1, the aircraft was operating in VMC in a region of weak vertical motion (see Fig. 6). At 18:54:33 UTC the aircraft entered what eventually became the first of three cumulus turrets in succession. Each turret appeared to be plumes originating or pulsing from an isolated 'hot spot', just west of the main cell. Maximum radar reflectivity with these cells was less than 15 *dBz*, as deduced from both airborne and ground based radars. Just prior to the first encounter, a fairly broad (~1 *km*) downdraft region was apparent from the *in situ* trace, as in most of the cases (see Fig. 6). The aircraft entered the plume and experienced a series of three updraft/downdraft pairs, each increasing in strength. The third plume exhibited an updraft/downdraft couplet with a horizontal wind shear in the vertical wind exceeding 12 ms^{-1} over 170 *m*. The gradient led to a normal load acceleration (Δn) of -0.81 *g*. The maximum RMS normal load ($\sigma_{\Delta n}$) during the event was 0.33 *g*, which is considered severe.[21,22]

Event 190.7

Event 190.7 was the strongest event of the day. Similar to Event 190.6, the aircraft encountered a region of relatively weak vertical motion before penetrating a growing cumulus updraft turret (see Fig. 7). The updraft had a width of about 750 meters with the peak updraft velocity located near the downwind side of the plume. The peak updraft velocity was 11.2 ms^{-1}. Within 1 second (~200 meters) the aircraft exited the plume and encountered a sharp downdraft of 6.23 ms^{-1}. The incurred peak load (Δn) measured during the event was –1.22 g and the RMS normal load ($\sigma_{\Delta n}$) peaked at just over 0.35, which again rates as a severe encounter. Consistent with 190.6, and as will be seen with the following day's severe encounters, the sharp gradient leading to the hazardous encounter was located downwind of the maximum updraft.

Flight 191

On December 14, 2000 the B-757 investigated a line of convection over Southern Georgia and the Florida Panhandle. This line was a remnant of the convective complex encountered on the previous day. However, it had now weakened and manifested itself as a narrow but nearly continuous line of convection extending northeastward from the Gulf (Figs. 8 and 9). The 1800 UTC National Weather Service surface analysis (Figure 8) showed an eastward moving low pressure in central Georgia with a cold front extending southwest into the Gulf of Mexico. The line of convection, which contained strong thunderstorms, was located about 100 *km* ahead of the surface cold front. Surface temperatures ahead of the line reached 80°F (27°C) in Tallahassee and were as cold as 35°F (2°C) in Jackson, Mississippi, which was about 300 *km* behind the cold front. In the 250 *mb* pressure surface analysis, an amplifying upper level trough and an associated jet stream maximum (65 ms^{-1}) centered over southern Missouri were driving the polar air mass behind the front southeast into the Gulf Coast States. Storm motion as deduced from TLH radar imagery was 13 ms^{-1} (25 *kts*) toward the northeast (from 240°), i.e. along the convective line.

The flight path relative to the TLH radar composite for Flight 191 is shown in Fig. 9. The aircraft flew within the cirrus outflow at the top of the thunderstorm line. Continuous turbulence was encountered while flying

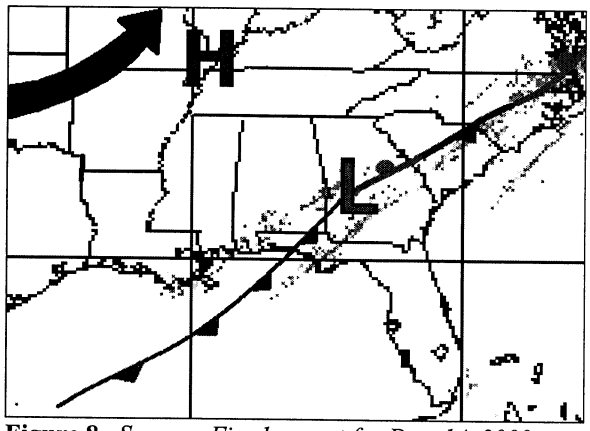

Figure 8. *Same as Fig. 1 except for Dec. 14, 2000.*

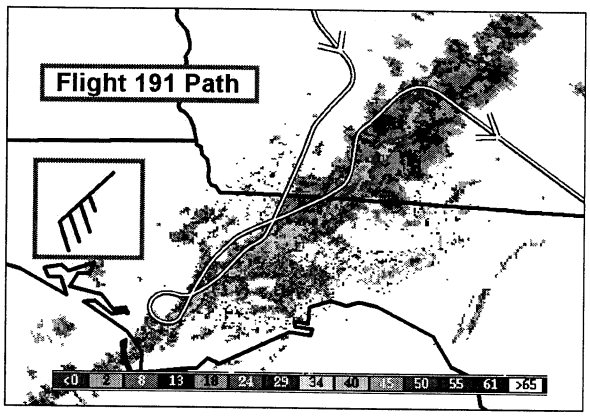

Figure 9. *Path of Flight 191 and ground based composite radar reflectivity (dBz) from the Tallahassee, FL radar at 18:44:21 UTC. Flight level wind vector (knots) is in the inset.*

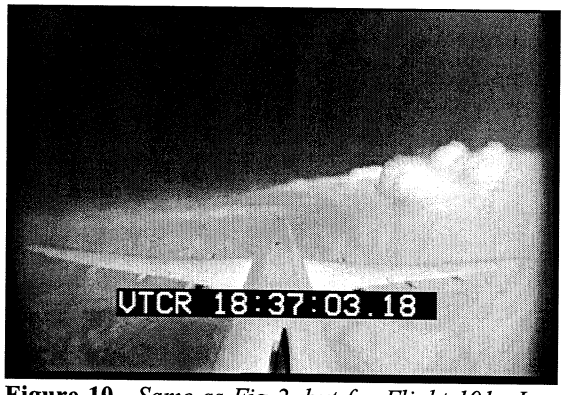

Figure 10. *Same as Fig 2, but for Flight 191. Image taken at 18:37:04.18 UTC, just prior to entering thunderstorm outflow region. Image is approximately 8 minutes prior to Event 191.3.*

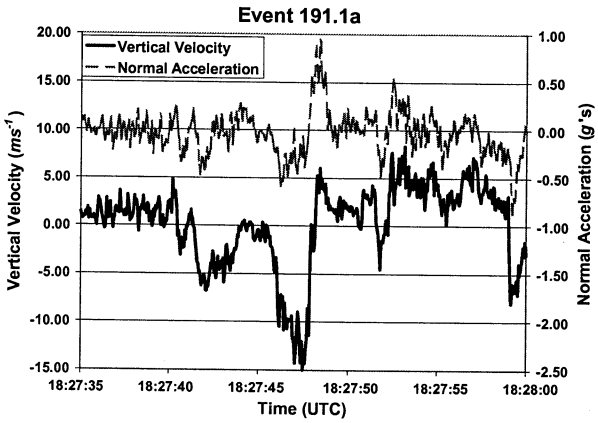

Figure 11. *Same as Fig. 3 but for Event 191.1a.*

within the outflow region. The strongest encounters were associated with the penetration of cumulus plumes that were rising through the outflow region. Figure 10 is a view from the onboard camera, looking up the thunderstorm line, prior to the penetration of the outflow region. After penetration, the aircraft remained in instrument meteorological conditions (IMC) providing few images from the onboard camera.

Event 191.1a

Event 191.1 was a relatively long, continuous turbulence event that is split into three subevents (see Table 2). During Event 191.1, peak airborne radar reflectivity ranged between 12 and 20 *dBz*. Unfortunately, TLH radar imagery at flight level was not available, since the aircraft flew almost directly over the radar site. This was the case for most of the events on this day. The first of the three subevents, 191.1a, was the strongest of the three, with an RMS normal load, $\sigma_{\Delta n}$ = 0.34 *g*. Similar to the severe encounters on the previous day (190.6 and 190.7), the aircraft while flying upwind experienced severe turbulence near the interface of a fairly broad (~1.5 *km*) downdraft (-15 ms^{-1}) located downwind of an updraft (6 ms^{-1}), as seen in Fig. 11.

Event 191.3

Event 191.3 (referred to as '191-06' in public forums[23] and in a companion paper[24]) occurred as the aircraft briefly encountered the northwestern edge of an isolated cumulus plume that was ascending through the outflow region. The event was characterized by continuous moderate levels of turbulence within the plume and a severe encounter upon exiting of the plume. This event was the strongest of all the events during the two flights. An RMS normal load ($\sigma_{\Delta n}$) of 0.44 *g* and corresponding peak normal loads (Δn) of +0.87 *g*/-1.4 *g*

were recorded (see Fig. 12). Similar to 190.6 and 190.7, the negative peak normal load occurred as the aircraft exited the plume on its downwind side (see circle indicating location of Event 191.3 in Fig. 13) into a fairly broad and intense region of downward motion. The aircraft descended 100 *m* before regaining its original flight altitude of 10.1 *km* MSL.

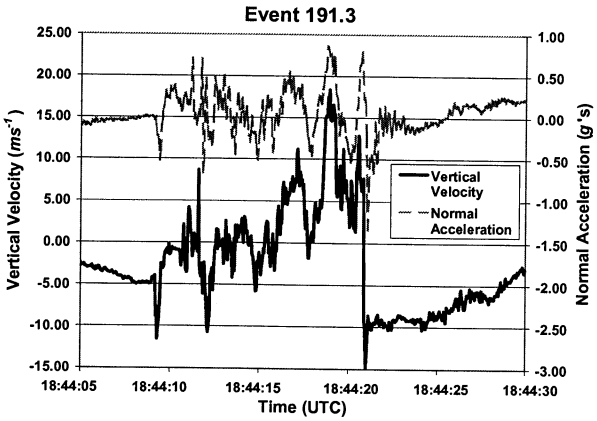

Figure 12. *Same as Fig. 3 but for Event 191.3.*

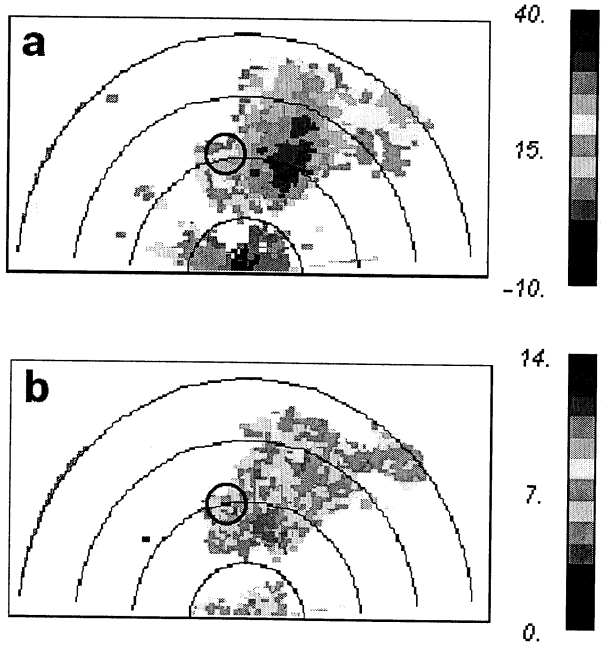

Figure 13. *Radar images from the B-757 onboard radar. Images are for (a) radar reflectivity (dBz) and (b) spectrum width (ms^{-1}). Black circle in both images denote the location of Event 191.3. Concentric circles are at 2 km intervals.*

Comparisons between the airborne and TLH radars for Event 191.3 are shown in Figs. 13 and 14. The ground based radar image in Fig. 14 is one minute before and about 400 *m* above the encounter. Along the path, the peak radar reflectivity from TLH imagery is nearly identical to that obtained from the airborne radar, i.e. 33 *dBz* (see Figs. 13a and 14a). Also, both radars show peak spectrum widths of 7 ms^{-1} on the downwind side of the plume (Figs. 13b and 14b). A spectrum width of this magnitude indicates severe turbulence[12].

This event, when compared to previous accident cases, was a fairly significant turbulence encounter. Figure 15 shows an analysis[25] of 52 turbulence encounters, some of which resulted in accidents. Included in the figure are the 18 significant encounters during the NASA flight experiments. In the figure, event 191.3 is represented as "NASA Flt* 191-06". The figure presents a comparison between the peak RMS normal

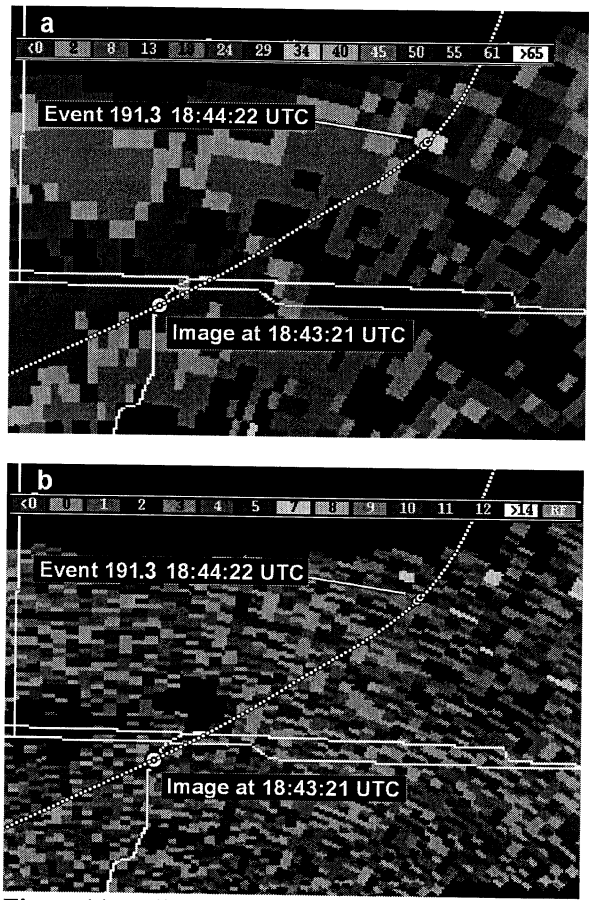

Figure 14. *Tallahassee, FL (TLH) ground radar images of (a) radar reflectivity (dBz) and (b) spectrum width in (ms^{-1}). Times for radar images and Event 191.3 position are denoted on the plots.*

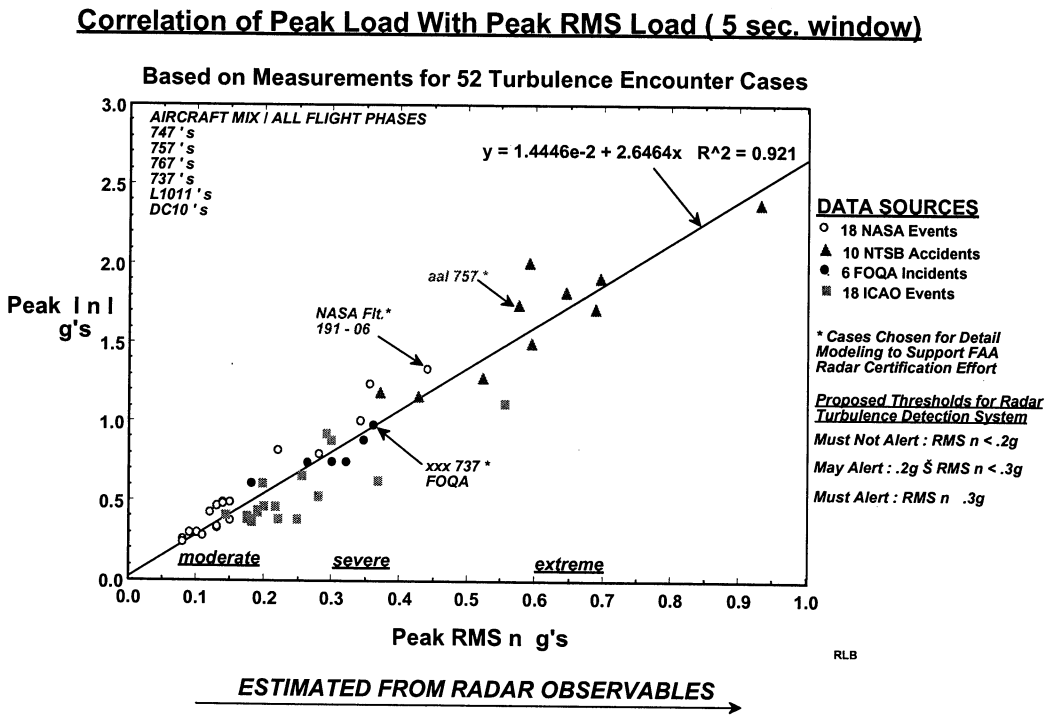

Figure 15. *Comparison of the radar estimated peak RMS normal load ($\sigma_{\Delta n}$) and the in situ measured peak load (Δn) for 52 Turbulence Encounter cases including the 18 NASA significant encounters. Image provided by Roland Bowles, AeroTech Research under NASA contract BPA-E03220D.*

loads and the peak normal loads (in the figure |n|) experienced by the aircraft. The figure clearly shows the severity of 191.3 when compared to other accident cases. In fact the peak load experienced during 191.3 ranks among National Transportation Safety Board (NTSB) accident cases (triangles in Figure 15).

Comparison Between the Two Flights

Figure 16 compares normalized vertical velocity structures of seven turbulence events. Fig. 16a shows three events when the aircraft flight path was orthogonal to the environmental wind vector and Fig. 16b shows four events when the aircraft flight path was along the environmental wind vector. When the flight path was orthogonal to the ambient wind vector (see Fig. 16a), the turbulence region in each event exhibited a symmetrical vertical velocity profile, i.e. a centered peak updraft and weak downdrafts on the periphery. On the contrary, when the flight path was along the ambient wind vector (see Fig. 16b), the turbulence region exhibited a nonsymmetrical vertical velocity profile. In each event, the peak updraft was located on the downwind side of the turbulence region. The peak downdraft was also located on the downwind side of the turbulence region. Furthermore, the peak normal load (Δn) occurred at the interface of these peak updrafts and downdrafts located on the downwind side of the turbulence region. All four turbulence events in Fig. 16b were severe while those in Fig. 16a were moderate.

In general, we found that turbulence was non-existent while flying in the clear air (VMC), but within the cloud (IMC) significant intensities of turbulence may occur. The turbulence encountered was characterized by a continuous spectrum of turbulence, e.g. Fig. 17.

Summary

Results from flight experiments that were conducted to test technologies to detect and warn of hazardous turbulence in convective environments have been presented. During the flights, the aircraft avoided high levels of radar reflectivity (> 35 dBz). Continuous turbulence was experienced while flying within convection and associated precipitation (IMC) but smooth conditions were present when flying outside of those

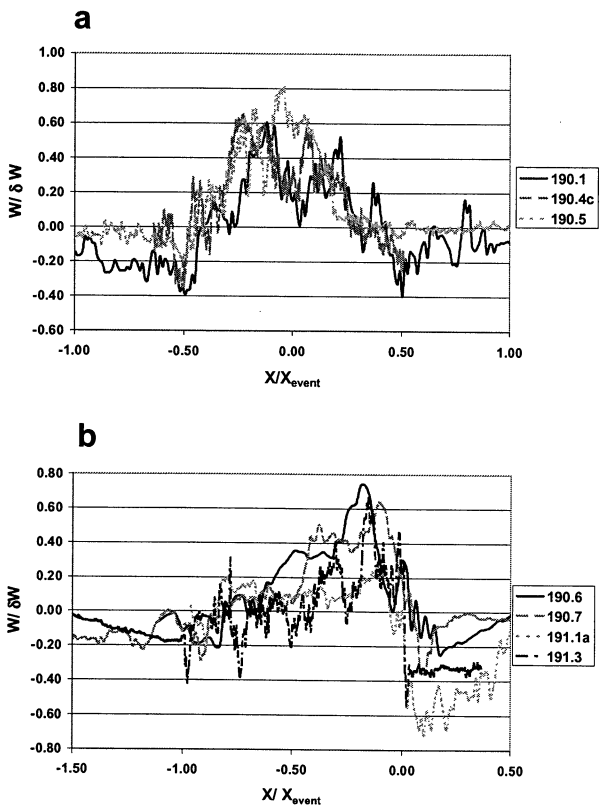

Figure 16. *Normalized vertical velocity from NASA in situ measurements when the aircraft path was (a) orthogonal to the environmental wind vector and (b) when the path was along the environmental wind vector. In (b) the environmental wind is from left to right. Distance (X) was normalized by the horizontal scale of the event. The vertical velocity was normalized by the change in the vertical velocity during the event.*

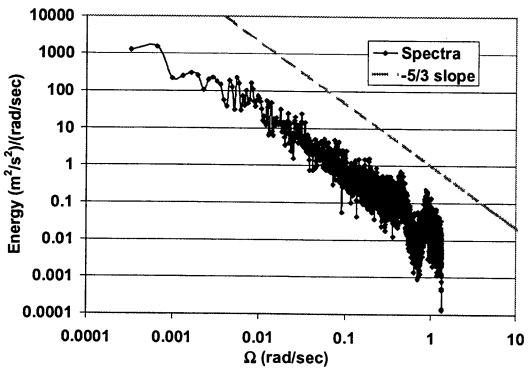

Figure 17. *Energy Spectra for Event 191.3. Energy is calculated from the in situ vertical winds during Event 191.3. Image provided by Paul Robinson, AeroTech Research, Inc. under NASA contract BPA-E03220D.*

regions (VMC). In all cases, radar reflectivity levels were low (< 35 *dBz*), and at times, lower than the detection ability of the airborne radar. However, the airborne radar did detect the hazardous turbulence along the flight path when radar reflectivity levels were relatively large, i.e. between 20 and 33 *dBz*.

All of the significant encounters with turbulence (moderate and above) where caused by the shear in the vertical wind that was located at the interfaces between updrafts and downdrafts. The most hazardous encounters occurred on the downwind side of rapidly growing cumulus turrets as the aircraft flew along the environmental wind vector. The most severe encounter with turbulence during the fall deployment was Event 191.3. Associated with Event 191.3 were horizontal changes in vertical winds of up to 27 ms^{-1} within a distance of 100 *m*. RMS normal loads ($\sigma_{\Delta n}$) of 0.44 *g* and peak normal load (Δn) of –1.4 *g* were associated with 191.3, and rank relatively high with regards to previous accident cases. Also, during 191.3, both ground-based and airborne radar spectrum width calculations predicted the severity of the turbulence encounter, which is consistent with previous experiments[12].

It is speculated by the authors that the factors that caused the turbulence during the NASA fall deployment could be considered as factors in previous turbulence accidents[2,5,8]. Similarities between the NASA flight experiments and reported accident accounts are as follows:

1) Event duration was typically less than 30 seconds and coincided with time spent within the cloud.
2) Consistent with pilot reports, events occurred inside cloudy regions where radar reflectivity levels were low (< 20 *dBz*). Furthermore, the events occurred outside of high reflectivity regions (> 35 *dBz*) associated with the most intense thunderstorm cells.
3) The most severe events occurred within the sharp gradient between a strong updraft and a downwind downdraft.

Acknowledgements

This research was sponsored by NASA's Aviation Safety Program. The authors would like to thank Paul Robinson and Roland Bowles of AeroTech Research, Inc for their contributions to this paper.

References

1. Kaplan, M.L., Lin, Y-L.,Riordan, A.J., Waight, K.T., Lux, K.M, and Huffman, A.W, "Flight Safety Characterization Studies, Part I: Turbulence Categorization Analyses," Interim Subcontrator Report to Research Triangle Institute, NASA contract NAS1-99074, October 1999.

2. Pantley, K. C., *Turbulence Near Thunderstorm Tops*, M.S. thesis, Department of Meteorology, San Jose State University, 1989, 132 pp.

3. Tolefson, H.B., "Preliminary Analysis of NACA Measurements of Atmospheric Turbulence within a Thunderstorm – U.S. Weather Bureau Thunderstorm Project," NACA TN 1233, 1947, 9pp.

4. Byers, H.R. and Braham, R.R., *The Thunderstorm*, Government Printing Office, 1949, 287 pp.

5. Wingrove, R. C. and Bach Jr, R. E., "Severe Turbulence and Maneuvering from Airline Flight Records," *J. Aircraft*, Vol. 31, 1994, pp. 753-760.

6. Ferris, R. F., "A Case Study of Mid-level Turbulence Outside Regions of Active Convection," Preprints, 8th Conference on Aviation, Range, and Aerospace Meteorology, Dallas, TX, Amer. Meteor. Soc., 1999, 5pp.

7. Burns, A., and Harrold, T. W., "An Atmospheric Disturbance Encountered by a Canberra Aircraft Over Storms at Oklahoma on 27th May 1965," R. Aircr. Establ. Tech. Rep. No. 66241, 1966, 20 pp.

8. Pantley, K. C. and Lester, P. F., "Observations of Severe Turbulence near Thunderstorm Tops," *J. of Applied Meteor.,* Vol. 29, 1990, pp. 1171-1179.

9. Press, H., and Binckley, E. T. "A Preliminary Evaluation of the Use of Ground Radar for the Avoidance of Turbulent Clouds," NACA TN 1684, 1948.

10. Thompson, J. K. and Lipscomb, V. W., "An Evaluation of the Use of Ground Radar for Avoiding Severe Turbulence Associated with Thunderstorms," NACA TN 1960, 1949, 10 pp.

11. Doviak, R. J. and Lee, J. T., "Radar for storm forecasting and weather hazard warning," *J. Aircraft*, Vol. 22, 1985, pp. 1059-1063.

12. Lee, J. T., "Application of Doppler Radar to Turbulence Measurements Which Affect Aircraft," Final Rep. No. FAA-RD-77-145. FAA Syst. Res. Dev. Serv., Washington, D.C., 1977.

13. Brewster, K.A., *Kinetic Energy Evolution in a Developing Severe Thunderstorm*, Master's Thesis, University of Oklahoma, Norman, 1984.

14. Bowles, R.L., "Theoretical Investigation of the Relationship between Airborne Radar Observables and Turbulence Induced Aircraft G-loads," AeroTech Report ATR-12007, (prepared for NASA Langley Research Center), October 1999.

15. Bowles, R.L., "Aircraft Centered Hazard Metric Based on Airborne Radar Turbulence Observables," AeroTech Report ATR-12010, (prepared for NASA Langley Research Center), September 2000.

16. Robinson, P.A. Buck, B.K., Bowles, R.L., Boyd, D.L.B., and Cornman, L.B., "Optimization of the NCAR In Situ Turbulence Measurement Algorithm," 38th Aerospace Sciences Meeting and Exhibit, AIAA 2000-0492, 10-13 January 2000, 8pp.

17. Benjamin, S.G., Grell, G.A., Brown, J.M., Brundage, K.J., Devenyi, D., Kim, D., Schwartz, B., Smirnova, T.G., Smith, T.L., Weygandt, S.S., and Manikin, G.A., "The 20-km Version of the Rapid Update Cycle," Preprints, 9th Conf. on Aviation, Range, and Aerospace Meteorology, Amer. Meteor. Soc., Orlando, 2000, pp. 421-423.

18. Nutter, P. A., and Manobianco, J., "Evaluation of the 29 km ETA Model. Part I: Objective Verification at Three Selective Stations. *Wea. and Forecasting*," Vol. 14, 1999, pp. 5-17.

19. Rogers, E., Black, T. L., Deaven, D. G., and DiMego, G. J.,: Changes to the Operational "Early" ETA Analysis/Forecast System at the National Centers for Environmental Prediction. *Wea. and Forecasting*, Vol. 11, 1996, pp. 391-403.

20. Kaplan, M. L., Lin, Y-L., Charney, J.J., Pfeiffer, K.D., DeCroix, D.S., and Weglarz, R.P., "A Terminal Area PBL Prediction System at Dallas-Fort Worth and its Application in Simulating Diurnal PBL Jets," *Bull. Amer. Meteor. Soc.,* Vol. 81, 2000, pp. 2179-2204.

21. Kessler, E., ed., *Thunderstorms: A Social, Scientific, and Technological Documentary. Vol. 1 – The Thunderstorm in Human Affairs*, 1981, U.S. Dept. of Comm., 206 pp.

22. Holcomb, M. C., "Jet Stream Analysis and Turbulence Forecasting," AFGWC TM 76-1, ADA062344, 1976, 101 pp.

23. Event 191.c was initially denoted as Event 191-06 by NASA contractor Aerotech, Inc. Presented as 191-06 during the NASA, 2nd Annual Weather Accident Prevention Project Review in Cleveland, Ohio, June 5-7, 2001.

24. Proctor, F.H., Hamilton, D.W., and Bowles, R.L., "Numerical Study of a Convective Turbulence Encounter," 40th Aerospace Sciences Meeting and Exhibit, AIAA 2002-0944, 13-17 January 2002, 14pp.

25. Bowles, R. L.: personal communication.